AIAA JOURNAL
Vol. 45, No. 5, May 2007

Optimization of Composite Laminates for Robust and Predictable Progressive Failure Response

Satchi Venkataraman* and Pablo Salas†
San Diego State University, San Diego, California 92118-1308

DOI: 10.2514/1.22077

Increasing robustness of structures with nonlinear history-dependent behavior requires their response to be very predictable. Predictability is made difficult by lack of good physical models (e.g., material failure), inaccurate analysis models, and insufficient resolution used in the discretized solutions. In complex structures, the problem is compounded by the complex interactions between the various individual failure events that happen at different scales. The systems that are highly nonlinear and exhibit competing failure paths are sensitive to small design variations and exhibit poor failure predictability. Small design variations significantly alter the failure paths in designs having competing failure modes, reducing predictability. Progressive failure of a composite laminate resembles complex systems with many failing components (plies) and multiple failure modes (plies can fail by shear, matrix, and/or fiber failure) that exhibit problems in failure predictability. In this paper, we investigate the robustness of energy absorption and predictability of the failure sequence of composite laminates in progressive failure response. This investigation demonstrates that deterministic optimization makes predictability poor due to the coalescence in failure modes. A traditional reliability optimization was performed to improve failure predictability. Analyzing designs obtained revealed that robust and predictable progressive failure requires the elimination of competing modes. Strain separation between successive failure modes was identified as a surrogate deterministic measure to eliminate competing failures. A deterministic optimization for maximizing energy absorption with a constraint for strain separation between successive failures in different modes was performed. The deterministic design obtained with the surrogate measure for predictability was comparable to the nondeterministic design in performance and predictability, indicating that this is a sufficient condition for improving predictability. The paper demonstrates an approach for investigating the mechanics that affect progressive failure predictability and developing simple and efficient surrogate measures to use in deterministic optimization to maximize performance and predictability.

Nomenclature

E	=	energy absorbed by a given design
$E_{\max}$	=	maximum energy absorbed by an optimized design
$E_{0.05}$	=	fifth percentile value of energy absorption
E_1	=	elastic modulus in the fiber direction
E_2	=	elastic modulus in the matrix direction
$F_1, F_2, F_{11}, F_{22}, F_{66}$	=	Tsai–Wu criterion constants
G_{12}	=	shear modulus of plies 1–2 planes
N_i	=	maximum load reached before failure at the ith failure event
N_x	=	normal force resultant in the x direction
N_{xy}	=	shear force resultant in the x–y plane
$P_{\Delta N}$	=	load drop penalty function
$(P_{\Delta N})_{\max}$	=	maximum value of the load drop penalty function
$P_{\Delta\varepsilon}$	=	strain separation penalty function
$(P_{\Delta\varepsilon})_{\max}$	=	maximum value of the strain separation penalty function
p_n	=	penalty parameter for load drop constraint
p_ε	=	penalty parameter for strain separation
ΔN_i	=	load drop at the ith failure event
$\Delta N_{\max}$	=	maximum allowed load drop at any failure event
$\Delta R_{\max}$	=	maximum relative load drop $\Delta N_i/N_i$ allowed at any failure event
$\Delta\varepsilon_{\min}$	=	minimum strain separation desired between failure events
ε_x	=	normal strain in the x direction
ε_x^i	=	strain at the ith failure event
θ	=	ply angle
κ_x	=	reference surface curvature in the x direction
κ_{xy}	=	reference surface twisting curvature in the x–y plane
κ_y	=	reference surface curvature in the y direction
ν_{12}	=	Poisson's ratio
σ_1	=	ply level stress along the fiber direction
σ_1^C	=	maximum compressive stress in the fiber direction
σ_1^T	=	maximum tensile stress in the fiber direction
σ_2	=	ply level stress transverse to the fiber direction
σ_2^C	=	maximum compressive stress in the matrix direction
σ_2^T	=	maximum tensile stress in the matrix direction
τ_{12}	=	ply level shear stress
τ_{12}^F	=	maximum shear stress in the 1–2 plane

Presented as Paper 2225 at the 46th AIAA/ASME/ASCE/AHS/ASC Structures, Structural Dynamics and Materials Conference 13th AIAA/ASME/AHS Adaptive Structures Conference, Austin, TX, 18–21 April 2005; received 27 December 2005; revision received 4 August 2006; accepted for publication 15 September 2006.

*Assistant Professor, Department of Aerospace Engineering and Engineering Mechanics, 5500 Campanile Drive, Mail Code 1308; satchi@mail.sdsu.edu. Member AIAA (corresponding author).

†Graduate Student, Department of Aerospace Engineering and Engineering Mechanics, 5500 Campanile Drive, Mail Code 1308. Member AIAA.

Introduction

IT IS highly desirable for engineering systems and structures to have a stable and predictable failure response. Increasing the complexity of engineering systems often also leads to complex failure behavior that has poor predictability and robustness. The lack of predictability here refers to the deviation of an actual failure sequence from the desired or designed failure sequence. The term

robustness is used as a measure of the variance of the system performance from its mean when subjected to small random variations in system variables. Numerous engineering accidents result from unexpected failures or failure responses. The tragic accident of the Space Shuttle *Columbia* was a reminder of how important it is to design systems that have a predictable failure response. Although the need for predictable failure is well accepted by engineers, at present, we have not established formal mathematical or numerical approaches to quantify and improve failure predictability by design optimization.

A study on the causes for poor predictability in complex systems (also called computability) by Belytschko and Mish [1] found that the primary contributors are the 1) lack of good analysis models that represent physical phenomena, 2) lack of affordable analysis capabilities for use in design, 3) insufficient resolution (temporal and spatial) used in numerical models, 4) complex and chaotic interactions between failure events, and 5) presence of competing failure modes and multiple bifurcation paths. The interaction in the failure events that leads to multiple bifurcations in failure response is a significant factor among many that affects predictability and robustness of progressive failure. In large or complex systems, the interaction between the coalesced failure modes and bifurcation events makes the design very sensitive to small changes in design or loading parameters and leads to very different failure paths.

Understanding the underlying mechanisms that create such bifurcations and competing failure paths, learning to control such bifurcations, and developing design optimization methods to introduce such control features to make failure predictable and robust will significantly advance the practice of design engineering. This research will facilitate the design of structural systems with robust and predictable (spatial and temporal) progression of damage or failure. This research has relevance to the optimal design of fail-safe structures, structural design for robust crashworthiness, and optimal and robust design of structures for progressive failure.

In this paper, we investigate factors that contribute to poor predictability in progressive failure response. The underlying physical mechanisms that lead to large deviations in the failure path when small variations are introduced to design variables and loading conditions are investigated. Understanding the factors that affect predictability makes it possible to develop methods to improve the predictability of failure.

Examples of Difficulty in Structural Progressive Failure Prediction

One example of difficulty in failure prediction is encountered in fully stressed designs and homogenous structures, for which predicting the exact failure initiation location can be challenging. Murri et al. [2] presented an example of fatigue life analysis of hybrid composite tapered flex beams. In this case, although it was possible to predict the crack growth accurately, it was not possible to predict the location and onset of the cracks. Failure predictability problems are often also encountered in the crash response of structures. Similarly, in the design of turbine blades, maximizing the stiffness and strength and minimizing weight often results in fully stressed designs for which it is difficult to predict the damage initiation site. Development of new material and manufacturing techniques such as functionally graded materials can be used more effectively if we can design for predictable failure initiation and progression (e.g., Vandeperre and Van Der Biest [3]).

Bifurcations in failure paths often lead to multiple competing failure paths. The Roux et al. [4] investigation of a head form impacting a pillar in an automotive crash analysis showed how small changes to design parameters trigger bifurcation modes that lead to large differences in the crash response. Lyle et al. [5] investigated the effect of various uncertainties on nonlinear transient response of the debris impact on the carbon–carbon leading edge of the space shuttle transport vehicle. The investigation revealed that the progressive failure response had multiple bifurcations that led to different failure paths having substantially different displacements and energy responses. Blumhardt [6] presented a crash example in which small

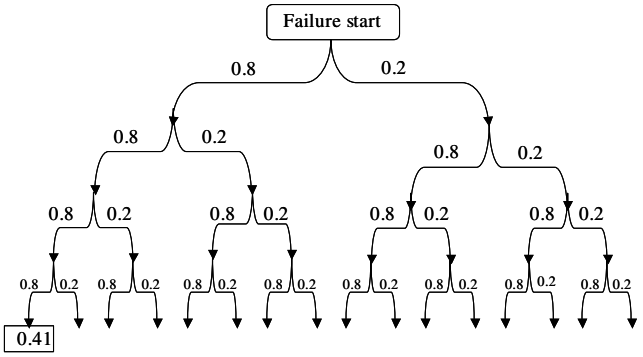

Fig. 1 The possible failure sequences in a progressive failure with four failure events and two competing modes at each failure (probability of desirable sequence is 41%).

design perturbations changed the buckling modes during crash and lead to very different crash response. Thole and Liguan [7] demonstrated that when the failure response has many such bifurcation events, small changes in the computing accuracy can change the nonlinear response significantly.

Predictability becomes an even greater issue for large, complex assemblies, because they are more prone to bifurcation events and exhibit complex interactions among these events. Complex engineering systems that exhibit multiple bifurcations in progressive failure can be described using failure event trees (Fig. 1). For the hypothetical system shown in the figure, at each bifurcation point there are two failure modes (a favorable and an unfavorable mode). At each bifurcation, the failure can choose one of the modes, due to the small stochastic variations in design parameters, geometry, loading, or material properties. Let us assume that the failure in the favorable mode (e.g., one that provides more energy absorption) is dominant (probability of 80%) compared with the less desirable or unfavorable failure path (probability of 20%). The probability of failure with the desired modes for a failure sequence with four bifurcation events is only 41%. If the number of failure sequences increases (e.g., to 10), then the design failure sequence has a probability of $(0.8)^{10}$, or 11%. This indicates that in complex systems, to achieve a reasonable probability for the desired failure sequence, it is necessary to design the system such that the failure in favorable modes has very high probabilities and further devise mechanisms to eliminate some or all undesired failure paths.

Large composite structures are examples of such complex systems. Failure predictability of composite structures in progressive failure and crash situations is significantly complicated, due to the large number of material failure modes they introduce, in addition to structural failure modes. Composite materials offer the advantage of light weight, high stiffness, and high strength properties and the increased design freedom to tailor properties. In crash applications, composite materials can increase energy absorption and dissipate a significant amount of the impact energy through material failure. These advantages are often offset by limitations introduced by the complexity of the material analysis, design, testing, and manufacture. In recent years, a great deal of effort has been invested in developing failure criteria, modeling, and analysis procedures for accurately predicting the failure of composite structures under nonlinear transient progressive failure conditions (Soden et al. [8]). Although efforts must continue toward developing such accurate analysis models and procedures, researchers must also investigate methods to make designs fail in a predictable manner.

Effect of Optimization on Failure Predictability

Deterministic optimization can further reduce the predictability of failure response in complex structures. When a structure is optimized, many failure modes that were originally well-separated in critical loads (hence their likelihood of occurrence) become less separated. The optimization process removes material that provides failure scenarios with large safety margins and employs it to increase the failure margin of failure scenarios with low safety margins. Thus,

perversely, the process of optimization increases the likelihood of a nonsimulated failure sequence manifesting itself in real life.

Examples of optimization making structural response more unpredictable have been demonstrated in shell buckling problems that are highly nonlinear and exhibit multiple bifurcations in their response. For cylindrical shells, it has been proven that optimization increases imperfection sensitivity. In the case of shells optimized for stability, optimization makes many different buckling modes possible at the critical load. This makes the design more sensitive to shape and thickness imperfections, resulting in an unexpectedly inferior design. Thompson and Supple [9] used a simple buckling structure to illustrate how the appearance of two or more failure modes simultaneously may affect the optimum solution by causing a nonlinear coupling of postbuckling modes that otherwise are stable (e.g., when acting separately). The buckling problem is solved analytically and numerically and it is shown that the optimum design's sensitivity to imperfections (which is directly related to the coalescence of failure modes) affects the postbuckling paths of the structure. That is, the optimization almost behaves as generator of imperfection sensitivity.

Designing for Failure Predictability

The idea of designing for predictability is a well-recognized concept that is applied in practice. Structural engineers have understood for years that in addition to superior performance, designs must have high predictability. Predicting failure of structures with homogeneous or uniform strength (fully stressed designs) is a challenging task, because it is difficult to predict the failure initiation site and hence failure progression. Engineers introduce features into the design to bias failure in certain modes can help improve failure predictability. For example, introducing a small curvature to a column loaded in compression will bias the buckling direction and will increase the predictability of the region in which the maximum stresses occur. There is evidence that nature uses this idea in the design of bones and other structural members. Bertram and Biewener [10] investigated the curvature present in long bones such as femurs and demonstrated that the curvature improves stress predictability. Because the optimum material microstructure of bone for compression and tension loading are significantly different (Reilly and Currey [11]), having high predictability of stresses is important.

For years engineers have designed structures that restrict their failure mechanisms or modes to those that can be analyzed. One such example is the design of structures for self-similar crack growth. There is no evidence that structures in which cracks can branch are inferior. Nevertheless, engineers continue to design structures such that any initial crack will grow in a self-similar manner, because branching cracks are difficult to analyze.

Engineers have also used weak points (structural fuses) to control failure sequences and enhance predictability. Structural fuses are features that produce large localized stress concentrations to initiate failure at that site, without altering the overall stiffness. A very simple example of structural fuse is the use of perforations in paper products such as toilet paper rolls and postage stamps. Because the paper is mostly homogeneous and can tear easily in any direction, perforations are introduced so that the paper will tear in a predictable and desirable fashion.

Structural fuses in the form of local dents, curvatures, or small initial cracks or slots have been used in structures in building implosions to design very precise and controlled failure sequences. The application of fuses is seen in the seismic design of steel deck-truss bridges for which the lateral bracing panels at supports are replaced with special ductile diaphragms to serve as fuses that protect the superstructure and substructure from damage during earthquakes (Sarraf and Bruneau [12]). Kim and Wierzbicki [13] demonstrated the use of structural fuses in the form of triggering dents in the car frames structure to improve crash performance. These dents initiate localized buckling leading to plastic failure at desired locations and provide a stable crash response.

Tailoring the load-deflection response of structures can provide more stable failure paths and therefore make the failure process more predictable. Pedersen [14] performed topology optimization of 2-D frame structures to follow prescribed load-deflection curve under progressive failure (energy absorption). The load-displacement response of 2-D frame was nonsmooth due to buckling of its members and the ensuing load redistribution, which posed numerical problems for the optimization. Pedersen introduced small curvatures into the truss members to overcome this difficulty. This was primarily done as a means to smooth the numerical response. However, the introduction of the small curvature into the truss members eliminated the bifurcation response and created a predictable load-displacement response for the truss members (subsystem).

Despite the numerous methods employed by engineers and designers to enhance failure sequence predictability, we are unaware of a formal design methodology for incorporating predictability as a design criterion. For complex problems, it is difficult or even impossible to identify a priori the failure paths that can provide good performance for crash protection and exhibit high predictability. Formal methodologies need to be developed to explore bifurcation paths, identify desirable paths, and introduce features to bias failure in such paths to simultaneously improve the predictability of performance and predictability in quantifiable ways.

Quantitative Methods for Improving Failure Predictability

Improving failure predictability could perhaps be achieved indirectly by formulating the problem as a probabilistic or nondeterministic design problem. In recent years, a great deal of effort and emphasis has gone toward developing nondeterministic design approaches such as reliability-based design optimization (RBDO). A large body of work exists in the area of reliability-based design optimization of structures. However, in progressive failure analysis of complex structures or systems, it is impossible to take into account all possible failure sequences and optimize for maximum reliability. Identifying the various failure mechanisms and failure sequences is a nontrivial task (Zimmerman and Corotis [15]). Often a subset of the dominant failure sequence is identified and the reliability for failure in those failure sequences is optimized (Mahadevan and Liu [16]). The shortcoming of this approach is that the optimization can turn failure sequences that were not dominant or active into dominant ones. Mahadevan and Liu [17] presented an approach for the probabilistic analysis of the ultimate failure load of a composite wing structure that included progressive failure analysis. The analysis requires identification of all possible failure sequences and the probability of failure along these sequences. To reduce the analysis computational effort, failure probability was calculated only for the dominant failure sequences.

For complex structures under progressive failure, calculating the probability of different failure sequences requires a large number of analyses, and is currently beyond our computational capabilities. Furthermore, as a structure is continuously changed during optimization, it is likely to transition from one failure sequence to another. The intermediate designs have poor predictability, because they can fail in both failure sequences. This results in optimal designs lying in disjoint design domains, which require special optimization tools (Cox et al. [18]).

The analysis of nonlinear history- and rate-dependent problems is difficult and computationally expensive [19]. Even with the most efficient methods available for RBDO, it is not possible to optimize complex structures that require nonlinear transient analyses [20]. Optimizing design variables in reliability-based optimization may not be able to increase predictability of crash response unless it can also eliminate the multiple failure paths and competing modes present in the complex failure response of the system.

Progressive Failure Analysis of Composite Laminates

Progressive failure of laminated composites resemble complex engineering design problems in that they have many failing components with multiple failure modes that can lead to competing failure modes/paths. However, progressive failure analysis of

laminated composites does not require computationally expensive analyses.

Composite laminates can carry substantial loads after the first ply failure event. When designed appropriately, the residual strength and stiffness of laminates loaded above the first ply failure limit can be significant. Determining the load-carrying capacity of the laminate from onset of material failure to ultimate collapse requires progressive failure analysis. In the progressive failure of a laminate, multiple plies fail progressively and each ply has several different modes of failure. For example, the ply can experience fiber failure, matrix failure, or fiber–matrix shear failure. As plies fail, the stiffness properties of the ply are degraded based on the failure mode detected and the laminate reaches ultimate failure when it has no stiffness left.

Remarkable advances have been made in recent years in the development of progressive failure analysis procedures and material degradation models for composite structures. However, structural design optimization procedures that provide prescribed damage field evolution or prescribed stiffness deterioration are still lacking.

Progressive Failure Predictability of Composite Laminates

Here we investigate the predictability of progressive failure sequence for composite laminates before and after optimization. The effects of small variations in design variables on the progressive failure response, namely energy dissipated during failure, and the progressive failure path (load versus strain and energy dissipated/absorbed versus strain) are investigated. Traditional measures of robust design are used to quantify predictability.

The progressive failure of a 48-ply symmetric and balanced composite laminate subjected to uniaxial tensile strain (Fig. 2) is chosen as an example to investigate failure predictability. A progressive failure analysis procedure was developed to compute the load versus strain history and energy dissipated by the progressive failure of the laminate plies. Classical lamination theory was used to calculate laminate strains and stresses [21]. The Tsai–Wu criterion [Eq. (1)] is used to predict failure of the plies [21]. For the predominant uniaxial loading this simple criterion has been shown to be reasonably accurate. The quadratic equation that represents the failure envelope for a lamina subjected to in-plane loads is as follows:

$$F_1\sigma_1 + F_2\sigma_2 + F_{11}\sigma_1^2 + F_{22}\sigma_2^2 + F_{66}\tau_{12}^2 - \sqrt{F_{11}F_{22}}\sigma_1\sigma_2 = 1$$
$$F_1 = \left(\frac{1}{\sigma_1^T} + \frac{1}{\sigma_1^C}\right), \qquad F_2 = \left(\frac{1}{\sigma_2^T} + \frac{1}{\sigma_2^C}\right), \qquad F_{11} = -\frac{1}{\sigma_1^T\sigma_1^C}$$
$$F_{22} = -\frac{1}{\sigma_2^T\sigma_2^C}, \qquad F_{66} = \left(\frac{1}{\tau_{12}^F}\right)^2 \tag{1}$$

The terms $\sigma_1, \sigma_2, \tau_{12}$ are the ply level stresses along fiber direction, transverse to fiber direction and in-plane shear stresses, respectively. The superscripts T and C denote tension and compression, respectively. If the stresses in the failure envelope equation are multiplied by a scale factor α, the equation reduces to a simple quadratic equation (2).

$$a\alpha^2 + b\alpha + c = 0 \Rightarrow \alpha = \frac{-b + \sqrt{b^2 - 4ac}}{2a}$$
$$a = F_{11}\sigma_1^2 + F_{22}\sigma_2^2 + F_{66}\tau_{12}^2 - \sqrt{F_{11}F_{22}}\sigma_1\sigma_2 \tag{2}$$
$$b = F_1\sigma_1 + F_2\sigma_2 \qquad c = -1$$

The positive root of the above quadratic equation α represents the critical load factor or safety factor and the ply with the smallest safety factor fails first [21]. The failure mode is determined by the largest absolute values among the three expressions in Eq. (3).

$$\text{fiber failure: } F_1\sigma_1 + F_{11}\sigma_1^2 \qquad \text{matrix failure: } F_2\sigma_2 + F_{22}\sigma_2^2$$
$$\text{shear failure: } F_{66}\tau_{12}^2 \tag{3}$$

A simple discrete ply discounting method [22,23] is used to degrade ply properties when failure is detected. For ply failure in shear failure mode, G_{12} and ν_{12} are degraded to 0.1 and 0, respectively; for ply matrix failure mode, E_2 and ν_{21} are reduced to 0.1 and zero, respectively; and for fiber failure mode, E_1, E_2, ν_{12}, and G_{12} are all reduced to zero. The general procedure used in the progressive failure analysis of the composite laminate is as follows. First, the laminate is loaded by strain increments until the first ply failure occurs (point A, Fig. 2). The stiffness of the failed plies is degraded using the discrete ply discounting method previously described. The stiffness reduction leads to change in ply stresses due to load redistribution. The plies are checked for failure. Any plies that fail are degraded and the procedure is repeated until no more plies fail. A new equilibrium point (point B, Fig. 2) is established after the series of stiffness degradations. Once the new equilibrium point is established, the loading is increased (segments B–C, Fig. 2) until the next ply failure occurs (point C, Fig. 2). At the next ply failure, the previous step is repeated until a new equilibrium point is found (point D, Fig. 2). This procedure continues until the laminate is unable to sustain any more strain increments without undergoing excessive deformation or there is no more load-carrying capacity left.

The energy dissipated during the progressive failure of the laminate is the area under the load-displacement curve in Fig. 2. The progressive failure analysis is performed by strain increments up to a maximum strain of 10% for all cases. The ply thickness is assumed to be 0.125 mm. We used the properties of AS4/3501-S graphite–epoxy material for our calculations. The stiffness properties and the maximum strengths of the ply materials are given in Tables 1 and 2.

In this study, we investigate the effect of small random variations of ply angles (design variables) on robustness of energy absorption and predictability of the failure sequence. The robustness is calculated by performing a Monte Carlo simulation [24]. The Monte Carlo simulation generates 1000 random variations of the design investigated in which the ply orientation angles are perturbed by a small amount. The ply angle variations in the laminate are random and uncorrelated and assumed to have a normal distribution with zero mean and standard deviation of 0.1 deg. The changes in the progressive failure response (failure sequence) are quantified by the changes in energy absorbed (or dissipated) during progressive failure. Statistical measures of the mean and standard deviation and the fifth percentile value of the energy absorbed are computed. The fifth percentile value of the energy absorption ($E_{0.05}$) corresponds to the fiftieth smallest energy absorption from the 1000 samples. This

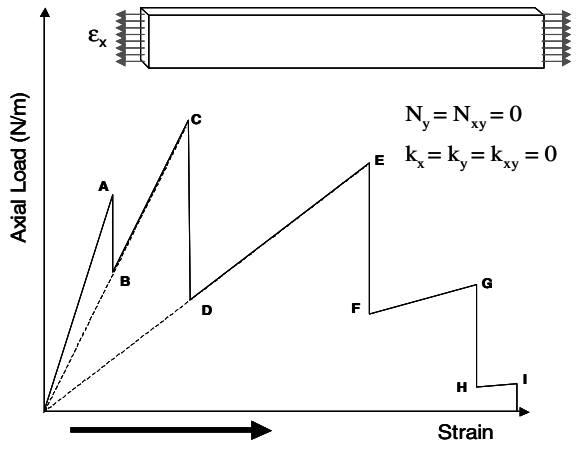

Fig. 2 Schematic of an axially loaded laminate with boundary conditions and its progressive failure response.

Table 1 Elastic properties of AS4/3501-S graphite-epoxy material

Elastic properties of the material	GPa
Elastic modulus in the fiber direction, E_1	126
Elastic modulus in the matrix direction, E_2	11
Poisson's ratio, ν_{12}	0.28
Shear modulus, G_{12}	91.5

Table 2 Maximum strengths of AS4/3501-S graphite–epoxy material

Maximum strengths of the material	Mpa
Maximum tensile stress in the fiber direction (σ_1^T)	1738.8
Maximum compressive stress in the fiber direction (σ_1^C)	1486.8
Maximum tensile stress in the matrix direction (σ_2^T)	48.4
Maximum compressive stress in the matrix direction (σ_2^C)	220
Maximum shear stress in the 1–2 plane (τ_{12}^T)	136

design will satisfy the requirement that the energy absorption will be greater than the $E_{0.05}$ ($E \geq E_{0.05}$) with 95% probability.

Progressive Failure Predictability of a Quasi-Isotropic Laminate

To establish a reference case, we perform progressive failure analysis of a 48-ply quasi-isotropic laminate with the ply stacking sequence $[(0/30/60/90/-60/-30)_4]_s$. Figure 3 shows the progressive failure response (load versus strain) for the quasi-isotropic composite laminate subjected to uniaxial strain. In Fig. 3, the progressive failure of the quasi-isotropic laminate without any ply angle variation (baseline design) is shown in the line with asterisk marks. The progressive failure of 100 laminates obtained by introducing small perturbations to the ply angles in the baseline design is shown in the solid lines. The random ply angle variations are assumed to have a normal distribution of zero mean and 0.1-deg standard deviation (i.e., 99% of ply angles are within ± 0.3 deg from their nominal values). When small random variations are introduced to ply angles, the designs take a slightly different path in progressive failure. However, the variability of the energy dissipated during failure remains small. It is also to be noted that the energy absorbed by the nominal design (design at mean values of the random variables) is lower than the mean value of the energy absorbed by the designs with imperfections.

Optimization of Laminate Stacking Sequence for Maximum Energy Absorption

One goal of this study is to understand the effect of deterministic optimization on predictability of the failure sequence. The ply stacking sequence of the laminate is optimized to maximize the energy absorption. A 48-ply laminate is restricted to be balanced and symmetric. The ply stacking sequence optimization is performed using a genetic algorithm developed by McMahon et al. [25]. The laminate representation is coded such that every ply of angle θ also has a $-\theta$ counterpart. Only one half is coded; the other half is generated by symmetry. The ply stacking sequence $[\pm\theta_1/\pm\theta_2/\ldots/\pm\theta_{11}/\pm\theta_{12}]_s$ optimization problem has 12 variables. The ply angles are restricted to a discrete set between 0 and 90 deg with 15-deg angle increments (seven possibilities). This makes the optimization an integer programming problem that has a total of 7^{12} possible discrete designs.

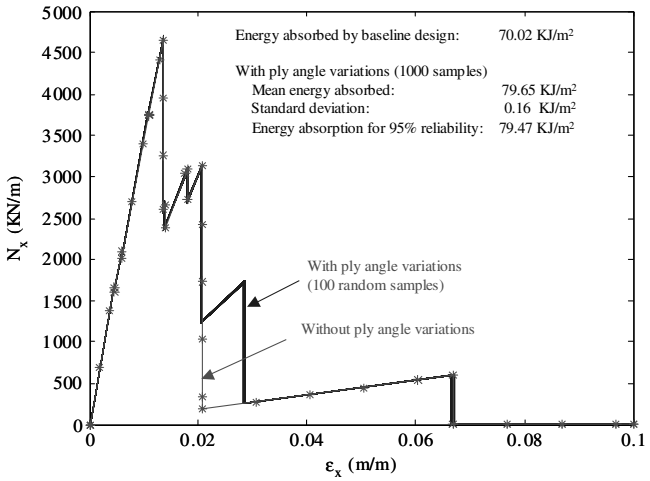

Fig. 3 Progressive failure (load versus strain) history for a quasi-isotropic $[(0/30/60/90/-60/-30)_4]_s$ laminate under uniaxial tension load.

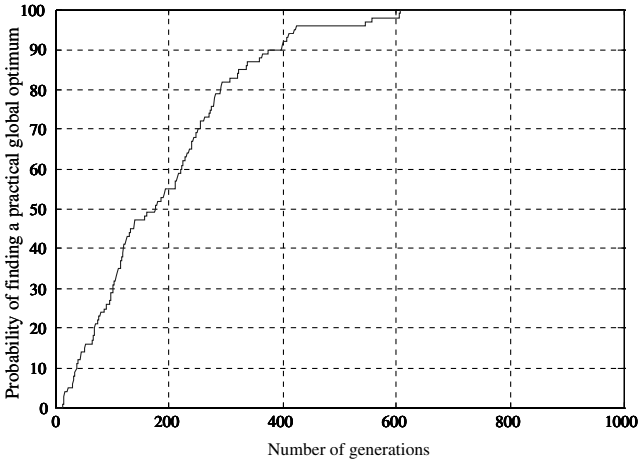

Fig. 4 Reliability of genetic algorithm with parameters tuned for the laminate optimization problem (calculated using 100 repetitions from random initial parent populations).

The following settings were used for the genetic algorithm used for a laminate ply stacking sequence. Population size is 25, number of generations is 1000, and number of repetitions from different random initial parent population is five. Two-point crossover uniform mutation operators were used for the optimization. Uniform mutation was used for the individuals' genetic changes. The probability of crossover was set equal to 100% (all the child individuals are created by two-point crossover operations) and the probability of mutation was set equal to 10% per chromosome. Permutation and swap operators do not have any effect in the optimization when the laminate is optimized for in-plane properties, therefore probabilities of zero were assigned to both of these operators. The crossover and mutation probabilities were adjusted by trial and error to increase the algorithm's reliability (see Fig. 4). Reliability is calculated as the fraction of the 100 repetitions in which we find a practical global optimum. For the actual optimization the genetic algorithm optimization was repeated five times from different starting populations and run for 1000 generations to increase the probability of finding a global optimum. Le Riche and Haftka [26] and Schutte and Haftka [27], demonstrate the advantage of repeating the searches from new starting populations to improve the reliability.

Progressive Failure of Laminate Optimized for Maximum Energy Absorption

The optimization for maximum energy absorption in progressive failure resulted in an optimum laminate design with stacking sequence $[\pm 15_7/\pm 30_4/\pm 45]_s$. The energy absorbed by the optimum design in progressive failure was 116.8 KJ/m^2. The predictability in the energy absorption of the optimum design is investigated by a Monte Carlo simulation of 1000 samples in which the ply angles of the laminates are subjected to variations that are normally distributed with zero mean and 0.1-deg standard deviation. The load versus strain history of the optimum design (line with asterisks) and 100 random samples of the optimum (solid lines) are plotted in Fig. 5. The statistics calculated from the Monte Carlo simulation are also indicated in the figure.

The failure paths of the optimum design were found to change significantly when the small ply angle variations (0.1 deg) are introduced. The progressive failure response of the design with small ply angle variations exhibits bifurcation in the failure paths leading to four different failure paths (Fig. 5). The mean value of the energy absorbed by the laminate significantly decreases when subjected to ply variations. The energy absorption that can be satisfied with 95% reliability (51 KJ/m^2) is less than half of the deterministic prediction for energy absorbed by the optimum design. This indicates that the deterministic design is highly sensitive to small variations in design variables.

The energy absorbed versus strain histories of the deterministic optimum design when analyzed with and without ply angle

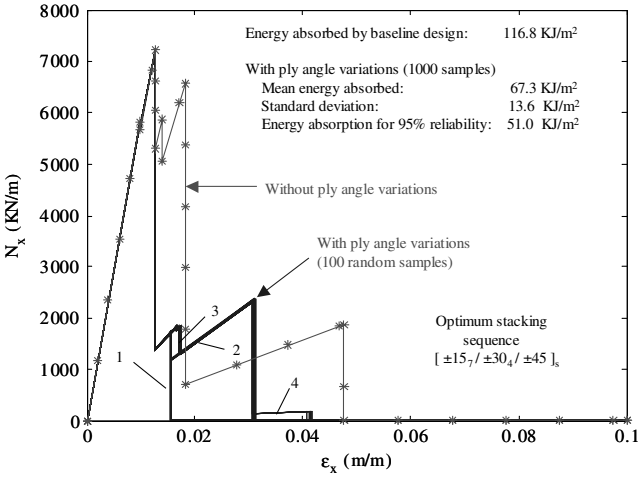

Fig. 5 Progressive failure history of the laminate optimized deterministically for maximum energy absorption under uniaxial tension load with and without ply angle imperfections.

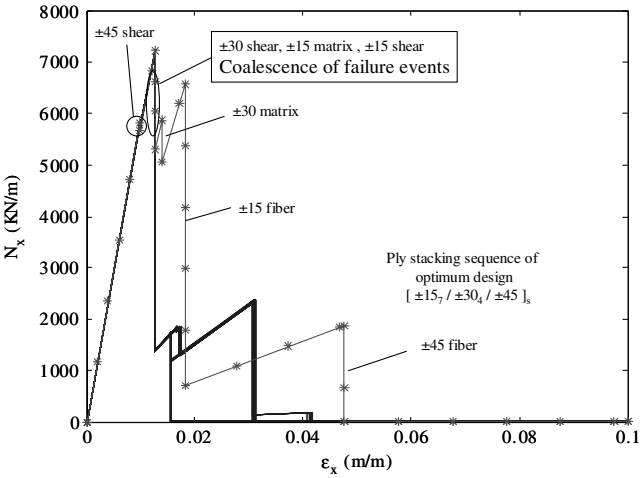

Fig. 7 Failure events at bifurcation points in the progressive failure response of the laminate optimized deterministically for maximum energy absorption.

variations are shown in Fig. 6. The energy versus strain plot reveals the bifurcation points in the progressive failure response leading to three distinctly different failure paths. The failure paths can be classified into two groups based on total energy absorbed.

Investigating the Cause for Bifurcations in the Progressive Failure Response

To identify and understand the mechanisms that lead to bifurcations in the failure response, the actual sequence of the failure events in the progressive failure of the optimum design is investigated. The failure events in the progressive failure of the optimum design without ply angle variations are shown in Fig. 7. The load and energy history reveal that the first bifurcation in the failure paths happens at a strain value of 0.012. Investigation of failure events shows that at this strain level there are multiple failure events happening in close succession: the shear failure of the 30-deg plies, matrix failure of 15-deg plies, and shear failure of the 15-deg plies. This coalescence of failure events to the same strain level is the underlying cause for the bifurcations that lead to very different failure paths.

A failure sequence comparison (see Table 3) reveals that in laminates with small ply angle variations, when plies of a given orientation fail (e.g., the $+30$ deg), the plies that provide the balance (the plies with the same but negative ply angles, e.g., -30 deg plies) do not fail. In the failure progression of the design without any random ply angle variations, the set of balanced plies fail simultaneously. This change in failure events is triggered by the asymmetry and unbalance in the laminate that result from the small

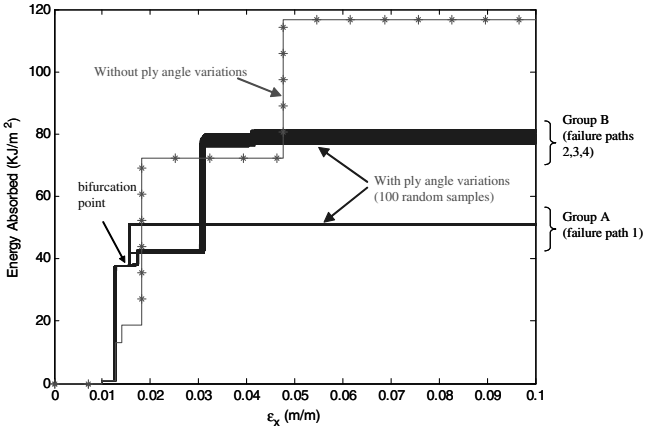

Fig. 6 Energy absorption during progressive failure of the laminate optimized deterministically for maximum energy absorption under uniaxial tension load.

random ply angle variations to the stacking sequence. The asymmetry of ply properties induces bending–extension coupling, and the unbalance induces shear–extension coupling [21]. Bending–extension coupling does not affect the progressive failure here, because the loading is specified as an enforced a pure in-plane strain state. However, it appears that the small increase in shear–extension coupling has a significant effect. The small increase in stresses due to the shear extensional coupling makes the laminate fail in the asymmetric pattern as discussed earlier. This further increases the shear–extension coupling and induces earlier fiber failure. For this example, the bifurcation ply failure stacking sequence predictability is affected mostly by the first bifurcation point in the failure path, caused by the coalesced failure modes.

For optimum energy absorption, plies must fail in the order of shear, matrix, and fiber failure modes, respectively (Table 3). The load-carrying capacity of the ply after shear is higher than that after matrix failure. The ply has no load-carrying capacity after fiber failure. When small ply angle variations are introduced, the resulting shear–extension coupling triggers fiber failure before it fails in the shear or matrix failure modes, thereby reducing the energy absorption. For example, in failure path 1, which leads to the lowest energy absorption, the 15- and 30-deg plies experience fiber failure mode before they can fail by the matrix or shear failure modes. Maximum energy occurs for the failure path that has the most failure events, because this allows for the most energy-dissipating mechanisms to occur.

The probability of failure events were computed for the 1000 samples analyzed with small ply angle imperfections. The failure sequence of the nominal design without imperfections is taken as a reference (Table 3, column 1). The probability that the failure modes at each event for design with imperfections follows the failure sequence of the nominal design without imperfections; namely, the 45 shear, 30 shear, 15 matrix, 15 shear, 30 matrix, 15 fiber, and 45 fiber failure modes are 100, 50, 35, 50, 10, 2, and 0%, respectively. This shows that the failure sequence has very poor predictability. The bifurcations along the path make the failure events later in the progressive failure history even less predictable.

To test the hypothesis that the changes in failure sequence are triggered by shear–extension coupling of the unbalanced laminate resulting from small ply angle variations, a Monte Carlo analysis is performed in which the laminate is perturbed by balanced random variations. Table 4 shows the comparison of the statistics of the Monte Carlo analysis with balanced and unbalanced ply orientation angle perturbations. The progressive failure behavior of the optimum laminate subjected to random but balanced ply angle variations is plotted in Fig. 8. When the ply angle variations are balanced, the bifurcation events that cause the different failure paths disappear and the progressive failure response becomes more predictable. The mean and fifth percentile value of energy absorbed (106.7 and

Table 3 Sequence of failure events in the various progressive failure paths of the optimum laminate

Failure path with no imperfections energy = 116.8 KJ/m^2		Failure path 1 with imperfections energy = 50.9 KJ/m^2		Failure path 2 with imperfections energy = 77.5 KJ/m^2		Failure path 3 with imperfections energy = 79.4 KJ/m^2		Failure path 4 with imperfections energy = 80.8 KJ/m^2	
Ply angle/ failure mode	No. of plies failing	Ply angle/ failure mode	No. of plies failing	Ply angle/ failure mode	No. of plies failing	Ply angle/ failure mode	No. of plies failing	Ply angle/ failure mode	No. of plies failing
±45/shear	2	±45/shear	2	±45/shear	2	±45/shear	2	±45/shear	2
±30/shear	8	+30/shear	8	−30/shear	8	−30/shear	8	+30/shear	8
±15/matrix	14	−15/matrix	14	+15/matrix	14	+15/matrix	14	−15/matrix	14
±15/shear	14	+15/matrix	4	−15/matrix	4	−15/matrix	4	+15/matrix	3
±30/matrix	8	+15/shear	10	−15/shear	10	−15/shear	10	+15/shear	11
±15/fiber	14	−30/shear	4	+30/shear	5	+30/shear	2	−30/shear	3
±45/fiber	2	+15/fiber	10	−15/fiber	10	−15/fiber	10	+15/fiber	11
		−30/shear	4	+30/shear	3	+30/shear	6	−30/shear	5
		−15/shear	14	+15/shear	14	+15/shear	14	−15/shear	14
		+15/fiber	3	−15/fiber	2	−15/fiber	2	+15/fiber	2
		+30/fiber	6	−30/fiber	7	−30/fiber	6	+30/fiber	6
		−45/matrix	2	+45/matrix	2	+45/fiber	1	−45/fiber	2
		+30/fiber	2	−30/fiber	1	−30/matrix	2	+30/matrix	2
		+15/fiber	1	−15/fiber	2	+45/fiber	1	+15/fiber	1
		±45/fiber	2	+45/fiber	2	−15/fiber	2	+45/matrix	2
		−30/matrix	8	−45/matrix	2	−45/matrix	2	+30/fiber	2
				−45/fiber	2	−30/fiber	2	−15/fiber	14
				+30/matrix	8	−45/fiber	2	−30/matrix	8
						+30/matrix	8		
Total no. of failures: 124			94		98		98		110

Table 4 Effect of small random ply angle variations on optimum design

Design with ply angle variations	Energy absorbed by design without ply angle variations	Statistics of energy absorption (KJ/m^2) with random normal ply angle variations having 0.1-deg standard deviation (1000 samples)		
		Mean	Standard deviation	Value for 95% reliability
Unbalanced	116.8	67.3	13.6	51.0
Balanced	116.8	106.71	1.33	104.6

104.6 KJ/m^2) are similar to that obtained for the design with no ply angle variations.

Optimization for Maximum Energy Absorption and Predictable Progressive Failure Response

The investigation of failure predictability in laminates optimized for maximum energy absorption indicates that multiple failures events at the same time or load level results in bifurcations in the failure path that lead to multiple competing failure paths. Small changes in design variables or loads change the order of failure events. Different failure modes result in different stiffness degradations. Therefore, even a small change in the order of failure events leads to a significant change in load distributions among the plies that leads to a different progressive failure response. In the presence of competing failure paths even small changes to design variables and loads lead to substantially different failure paths and energy absorptions. Bifurcations in failure response and the resulting competing failure paths can be eliminated if the competing failure events can be eliminated. This means that coalescence of failure events to the same strain level during optimization has to be avoided. Eliminating bifurcations leads to predictable failure sequences and robust energy absorption in progressive failure. In this section, we investigate strategies to optimize laminates for maximum energy absorption with constraints to prevent coalescence of failure events to the same strain level. The designs are compared with optimum designs obtained from traditional reliability-based optimization.

Maximization of Energy Absorption with Constraints for Separation Between Progressive Failure Events

The load versus strain behavior in progressive failure indicates that when many plies fail simultaneously at a given strain level, there is a large reduction in the load resultant (Fig. 9). Minimizing load reduction caused by ply failure events will result in a laminate when fewer plies fail at any strain level. From here on, we will refer to this approach as minimizing the *load drop*. Similarly, maximizing the strain increments (loading) between successive ply failure events can also minimize the coalescence of multiple failure events to the same strain level. We will refer to this approach as *strain separation between ply failure events*.

Minimizing load drop and maximizing strain separation will ensure that after each failure the laminate stiffness will not degrade by a large amount and that the laminate can be subjected to strain

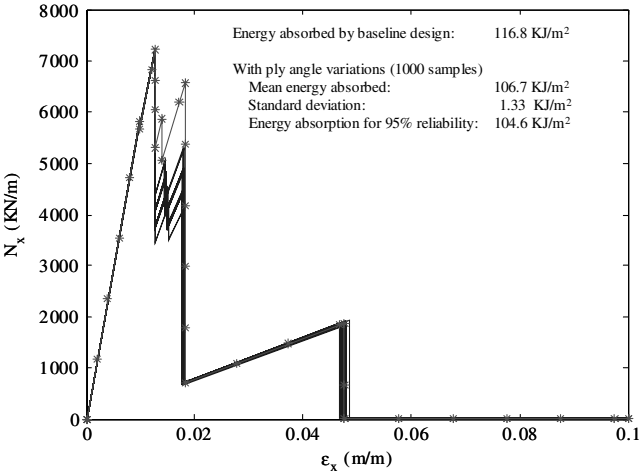

Fig. 8 Progressive failure response of the laminate optimized for maximum energy absorption when subjected to balanced ply angle variations.

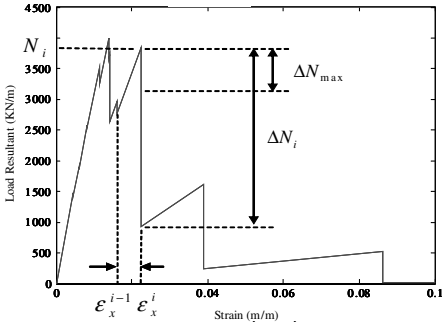

Fig. 9 Schematic showing the constraints imposed on the load drop and strain separation between ply failure events to obtain design with failure separation.

increments before the additional ply failures occur. Simultaneously maximizing energy absorption (performance) and maximizing separation between failure events to increase predictability represents a multi-objective optimization problem that can be converted to a single objective optimization for maximizing energy absorption with constraints on maximum load drop and for minimum strain separation. The constraints are introduced into the genetic algorithm as penalty functions added to the energy absorption. The objective function used for optimization with penalty functions for load drop constraints ($P_{\Delta N}$) and strain separation ($P_{\Delta\varepsilon}$) is as follows:

$$\text{maximize}\left[\frac{E}{E_{\max}} - \frac{P_{\Delta N}}{(P_{\Delta N})_{\max}} - \frac{P_{\Delta\varepsilon}}{(P_{\Delta\varepsilon})_{\max}}\right] \tag{4}$$

Penalty Function for Limiting Load Drop at Ply Failure Events

The constraint on the load drop due to failure can be specified to be less than some absolute value of load drop or it can be specified to be a fraction of the current load level. The penalty function is computed by summing contributions from all ply failue events that violate the specified constraint on the load drop. The penalty functions for load drop based on absolute and relative value are as follows:

$$P_{\Delta N} = \sum_{i=1}^{n} p_n \left\langle \frac{\Delta N_i}{\Delta N_{\max}} - 1 \right\rangle \tag{5}$$

$$P_{\Delta N} = \sum_{i=1}^{n} p_n \left\langle \frac{\Delta N_i}{N_i \Delta R_{\max}} - 1 \right\rangle \tag{6}$$

where ΔN_i is the load drop at the ith ply failure event, N_i is the maximum load reached before failure at the ith ply failure event, $\Delta N_{\max}$ is the maximum allowed load drop at any ply failure event, $\Delta R_{\max}$ is the maximum relative load drop $\Delta N_i/N_i$ allowed at any ply failure event, p_n is the penalty parameter for load drop constraint and the operand $\langle a\rangle = \frac{1}{2}(a + |a|)$. The values of $\Delta N_{\max} = 3000$ KN/m and $\Delta R_{\max} = 20\%$ were used for the optimization. The $(P_{\Delta N})_{\max}$ term is used to scale the penalty function $P_{\Delta N}$, and it is calculated by maximizing $P_{\Delta N}$ using the GA (it was found to have a value of 85.94):

$$(P_{\Delta N})_{\max} = \max\left\{\sum_{i=1}^{n}\left\langle \frac{\Delta N_i}{N_i \Delta R_{\max}} - 1 \right\rangle\right\} \tag{7}$$

Enforcing Strain Separations Between Ply Failure Events

The strain separation constraint specifies that the difference in strains between any two consecutive ply failures have to be greater than a specified minimum strain increment. The penalty function used to enforce this constraint is as follows:

$$P_{\Delta\varepsilon} = \sum_{i=1}^{n} p_\varepsilon \left\langle 1 - \left(\frac{\varepsilon_x^i - \varepsilon_x^{i-1}}{\Delta\varepsilon_{\min}}\right)\right\rangle \tag{8}$$

where, ε_x^i is the strain at the ith ply failure event, $\Delta\varepsilon_{\min}$ is the minimum strain separation desired between ply failure events (0.001 for this study), and p_ε is the penalty parameter for strain separation. As before, the term $(P_{\Delta\varepsilon})_{\max}$ is calculated as follows:

$$(P_{\Delta\varepsilon})_{\max} = \max\left\{\sum_{i=1}^{n}\left\langle 1 - \left(\frac{\varepsilon_x^i - \varepsilon_x^{i-1}}{\Delta\varepsilon_{\min}}\right)\right\rangle\right\} \tag{9}$$

where the value of $(P_{\Delta\varepsilon})_{\max} = 31.67$ was used for the optimization.

Laminates Optimized for Energy Absorption with Strain Separation Between Ply Failure Events

The penalty parameters shown were obtained by trial and error to achieve a balance between maximizing energy absorption and improving failure predictability. The sensitivity of the final designs or the optimization convergence to these parameters was not investigated. The designs obtained from optimization for different penalty functions are presented in Table 5. The energy absorption of the optimum designs without any random ply angle variations is presented. For each design we perform a Monte Carlo simulation in which ply angle variations with zero mean and standard deviations of (0.1, 0.2, 0.3, 1.0, and 1.66 deg) are introduced. The 95th percentile value (50th smallest) of the energy absorbed from the 1000 samples is reported for each Monte Carlo analysis.

The optimum design obtained with absolute and relative load drop constraints were ineffective in eliminating competing modes (Table 5). The strain separation method was effective in reducing failure coalescence in optimization and resulted in an optimum design that exhibited fewer competing failure paths (Fig. 10). The statistics shown on Fig. 10 indicate that strain separation was effective in reducing the variability of the energy absorption response (low standard deviation). The energy absorbed by the design is 95.6 KJ/m^2, which is lower than that of the optimum design obtained without any strain separation (116.8 KJ/m^2). The energy absorption of the laminate optimized only for maximum energy absorption exhibits large sensitivity to small ply angle

Table 5 Comparison of optimum designs obtained using deterministic optimization with different penalty functions for failure mode separation

Optimization criterion, penalty parameters, and optimum ply stacking sequence	Energy absorbed by design	Energy absorption limit (KJ/m^2) for 95% reliability under random normal ply orientation angle variations with standard deviation of				
	KJ/m^2	0.1 deg	0.2 deg	0.3 deg	1.0 deg	1.66 deg
Maximum energy absorption $[\pm\mathbf{15_7}/\pm\mathbf{30_4}/\pm\mathbf{45}]_s$	116.8	51.0	50.9	50.3	47.5	47.5
Mode separation using relative load drop penalty ($p_n = 1$ and $p_\varepsilon = 0$) $[\mathbf{0_6}/\pm\mathbf{15_2}/\pm\mathbf{30_5}/\pm\mathbf{45}/\pm\mathbf{60}]_s$	93.1	65.4	64.7	64.0	60.9	59.9
Mode separation using strain separation penalty ($p_n = 0$ and $p_\varepsilon = 0.5$) $[\mathbf{0_{12}}/\pm\mathbf{30_4}/\pm\mathbf{60}/\pm\mathbf{90_2}]_s$	95.6	87.1	86.6	86.1	82.6	80.6
Mode separation using strain separation and absolute load drop penalty. ($p_n = 1$ and $p_\varepsilon = 1$) $[\mathbf{0_6}/\pm\mathbf{15_3}/\pm\mathbf{30_4}/\pm\mathbf{60}/\pm\mathbf{90_2}]_s$	91.5	83.0	82.4	81.8	77.4	76.3
Mode separation using strain separation and absolute load drop penalty. ($p_n = 1$ and $p_\varepsilon = 1$) $[\mathbf{0_8}/\pm\mathbf{15_3}/\pm\mathbf{30_2}/\pm\mathbf{45}/\pm\mathbf{60}/\pm\mathbf{90_2}]_s$	86.7	81.4	81.0	80.7	79.0	77.6

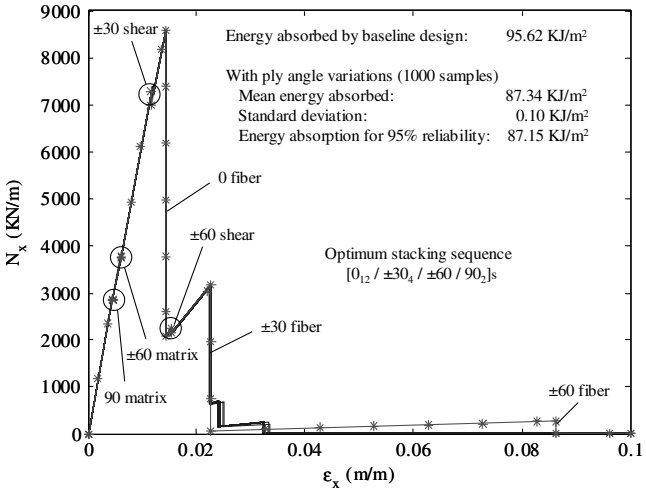

Fig. 10 Progressive failure of laminate optimized with strain separation between ply failure events when analyzed with and without ply angle variations.

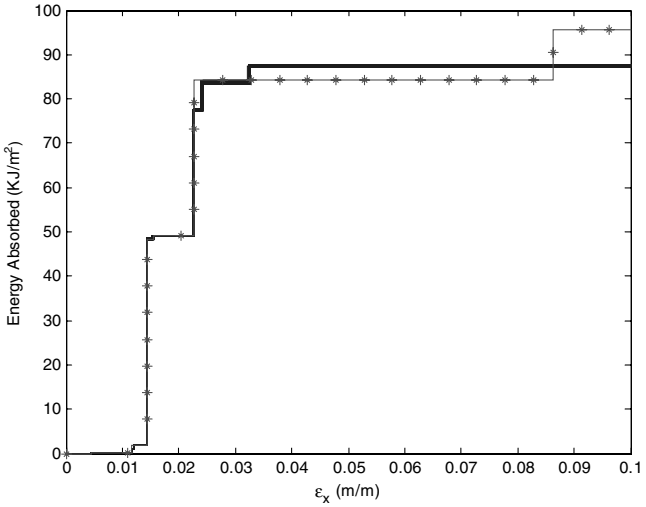

Fig. 11 Energy absorbed during progressive failure by the laminate optimized with strain separation between ply failure events when analyzed with and without ply angle variations.

variations. The Monte Carlo simulation of the optimum design showed that the mean energy absorption decreased by 42%, and the energy absorption limit for 95% reliability decreased by 56% when ply angle variations of 0.1-deg standard deviation were introduced. The optimization for maximum energy with constraints for strain separation provides an optimum design that absorbs 87.15 KJ/m^2 with 95% reliability (only 9% lower than the deterministic value) when subjected to random ply angle variations of 0.1-deg standard deviation.

The energy absorption history plots (Fig. 11) indicate that separating failure events using strain separation was successful in eliminating bifurcations in the failure path. Increasing the standard deviations of the ply angle variations from 0.1 to 1.0 deg (a factor of 10) resulted in a 13% decrease in the energy absorption limit for 95% reliability to 82.6 KJ/m^2 compared with the case with no ply angle variations, and 5% compared with the case with ply angle variations of 0.1-deg standard deviation.

Investigating the failure events of the optimum design with strain separation indicates that at any strain level at which failure occurs there is only one failure mode at each failure event. In other words, at any strain level for which failure occurs, plies of different orientations do not fail, and plies of the same orientation fail in exactly identical failure modes. A comparison of the performances is summarized in Table 6. This demonstrates that by controlling and/or eliminating bifurcations in failure paths, we can effectively eliminate the competing failure paths and improve robustness using deterministic optimization methods. The energy absorption of the design with strain separation when subjected to small random ply variations still decreases by a small amount compared with the deterministic prediction (however, it is desirable to keep this reduction small). This indicates that there is more room for improving failure predictability for the laminate progressive failure. In the next section, we perform a reliability-based optimization that maximizes the 95th percentile value for energy absorption. The predictability of the design obtained from the reliability-based optimization will be compared with the deterministic design obtained with constraints for failure event separation.

Reliability Optimization of Energy Absorption in Laminate During Progressive Failure

The effectiveness of separating ply failure events to eliminate competing failure modes and thereby improve robustness and reliability of progressive failure response was demonstrated. The fifth percentile value of the energy absorption of the designs from a Monte Carlo simulation was used as a measure of the robustness of the optimum design. In a traditional probabilistic method that measure becomes the objective function. The simplicity of this problem allows us to perform this optimization, which requires a very large number of design evaluations. The objective of this study is to compare the designs obtained from deterministic optimization with failure mode separations with those obtained using the traditional nondeterministic approach. The reliability optimization is used to maximize the energy absorption limit that will provide 95% reliability in the presence of small random ply angle variations. Therefore, the optimization becomes the maximization of the fifth percentile value of energy absorption among the 1000 Monte Carlo samples analyzed. The optimization problem statement is the following:

$$\text{maximize } E_{0.05} \tag{10}$$

The reliability analysis is performed using a Monte Carlo analysis of 100 samples. The sample size is reduced from the 1000 size used for analysis before to reduce computational effort. A convergence analysis indicated that the error in the fifth percentile value of energy absorption from a sample size of 100 is less that 1% compared with those obtained from a sample size of 1000 (Table 7). The optimum designs obtained for ply angle variations of 0.1-, 0.2-, and 1.0-deg standard deviation are shown in Table 8.

Table 6 Comparison of optimum designs obtained using deterministic optimization without and with failure mode separation

Optimal design	Energy absorbed by design without ply angle perturbations, KJ/m^2	Energy absorbed by design with ply angle perturbations (1000 random samples with ply angles having normal distribution and 0.1-deg standard deviation, KJ/m^2		
		Mean	Standard deviation	Energy absorbed with 95% reliability
Deterministic design with no mode separation	116.8	67.3	13.6	51.0
With strain separation	95.6	87.3	0.10	87.15
With strain separation and load drop penalty	86.7	81.4	0.15	81.3

Table 7 Effect of sample size on convergence of the fifth percentile energy absorption value obtained from the Monte Carlo simulation. The stacking sequence of the design analyzed for is $[0_8/\pm 15_3/\pm 30_2/\pm 45/\pm 60/90_2]_s$

Sample size of	Energy absorption limit (KJ/m^2) for 95% reliability when analyzed for ply orientation angle variations of 0.1-deg standard deviation										Average error with respect to the 1000 sample size, %
100	78.06	77.91	78.06	78.11	78.04	78.15	77.86	78.21	78.05	77.76	0.12
200	78.01	78.09	78.11	77.93	77.97						0.08
500	78.06	78.04									0.1
1000	78.05										

Table 8 Optimum designs obtained using reliability-based optimization for angle variations and their performance when analyzed at other larger values of ply angle variations

Standard deviation of ply angle variations used for reliability optimization	Optimum stacking sequence	Energy absorbed by baseline design, KJ/m^2	Energy absorption limit (KJ/m^2) for 95% reliability when analyzed for ply orientation angle variations of				
			0.1 deg	0.2 deg	0.3 deg	1.0 deg	1.66 deg
0.1 deg	$[\mathbf{0_6}/\pm\mathbf{30_6}/\pm\mathbf{45_2}/\pm\mathbf{60}]_s$	115.3	109.7 (111.2, 0.89)[a]	65.7	64.2	58.9	56.9
0.2 deg	$[\mathbf{0_2}/\pm\mathbf{30_3}/\pm\mathbf{45_3}/\pm\mathbf{60_2}/\pm\mathbf{75_2}/\pm\mathbf{90_2}]_s$	83.0	98.6 (99.2, 0.29)[a]	97.4	95.3	75.7	69.9
1.0 deg	$[\mathbf{0_{18}}/\pm\mathbf{30}/\pm\mathbf{45}/\pm\mathbf{60}]_s$	90.2	9.35 (93.7, 0.09)[a]	93.1	92.7	90.5	89.3

[a]Values in parenthesis are the mean and standard deviation of the energy absorbed by the laminates with small random ply angle variation.

The fifth percentile value of energy absorption for the reliability-based optimum designed for 0.1-deg ply angle variations was 109.7 KJ/m^2. This is significantly larger than the 95% reliability limit for energy absorbed by the deterministic optimum design with strain separation, which absorbed 87.3 KJ/m^2. Figure 12 shows the progressive failure of the design optimized and analyzed for 0.1-deg standard deviation in ply angle variations. The progressive failures of the designs with and without ply angle variations are almost identical. Investigation of the failure events indicates that the reliability optimization did not fully eliminate competing failure modes. When the design optimized for random ply angle variations with 0.1-deg standard deviation is subjected to larger ply angle variations of 0.2-deg standard deviation, the progressive failure exhibits bifurcations. The energy absorbed with 95% reliability for the increased ply angle variations is only 65.7 KJ/m^2. Figure 13 shows the progressive failure of the reliability-based optimum design for 0.1-deg ply angle variation analyzed with 0.2-deg ply angle variations. When subjected to increased ply angle variations, the strains levels that exhibited competing failure modes (Fig. 12) lead to bifurcations that result in competing failure paths that provide very different energy absorption. Reliability optimization with large ply angle variations of 1.0-deg standard deviation was successful in obtaining a design with no competing failure modes and a high energy absorption with 95% reliability value (93.5 KJ/m^2).

Reliability optimization for small ply angle variations did not completely eliminate the competing failure modes (even very small changes lead to different failure paths). On the other hand, reliability optimization for large ply angle variations was successful in eliminating competing failure modes thereby making the design predictable (robust) with a high energy absorption value (performance). However, the design does have coincident failure modes. This indicates that the strain separation condition may be a sufficient condition, but not a necessary condition for failure predictability. The reliability optimization procedure required 7.5×10^6 analyses (100 laminate analyses for each reliability calculation and 75,000 reliability analyses for each optimization). For the reliability optimization, the GA was repeated 3 times using a population size of 25 for 1000 generations. The large number of analyses is a result of probability measures using Monte Carlo simulations within the global optimization loop. Such optimizations can only be performed with very simple examples such as the laminate used here and will be prohibitively expensive to attempt for real crash or nonlinear buckling examples.

Comparing the best deterministic design including failure mode separation with the best reliability design indicates that the formulation for failure mode separation penalty approach needs revision. In the current optimization approach we penalize the design when multiple plies fail at the same strain level. However, it is not the

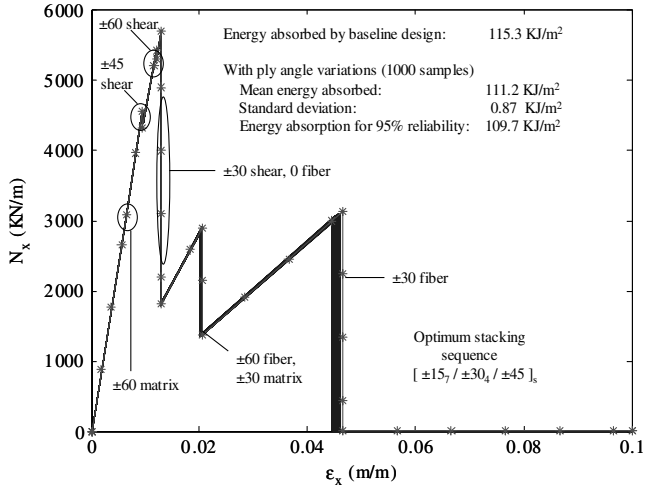

Fig. 12 Progressive failure of laminate obtained using reliability optimization when analyzed with ply angle variations of 0.1-deg standard deviation.

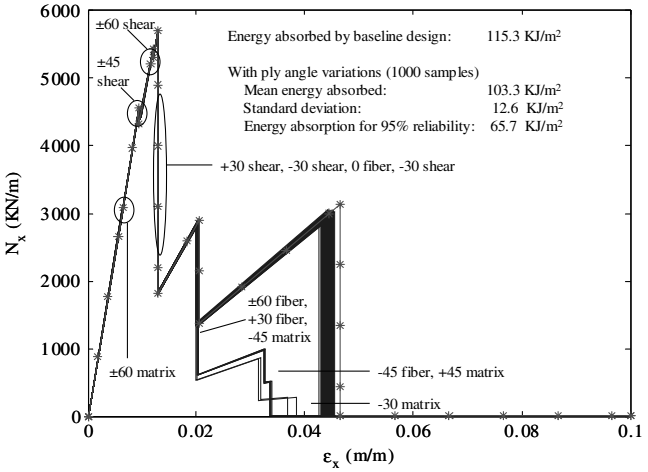

Fig. 13 Progressive failure of laminate obtained using reliability optimization when analyzed with ply angle variations of 0.2-deg standard deviation.

number of plies that fail that matters. Rather, the competing failure paths are created by the plies failing through different failure modes at a given strain level. The penalty function for strain separation should be modified such that the laminate energy absorption is penalized if plies of different orientations fail at the same strain level (regardless of the failure mode) or if plies of the same orientation fail in different modes at the same strain level.

The optimization also revealed that maximum energy absorption occurs when all plies of the laminate fail in all three modes in the order of shear, matrix, and fiber, respectively. This is the optimum failure sequence needed for maximizing performance. If we can find designs that fail in this sequence and optimize them to minimize competing failure modes, we can obtain an optimum design that has high predictability and performance. A two-level optimization can be designed in which the lower-level laminate ply orientations are optimized to cause failure in the specified sequence, and at the upper level, the reliability of the designs is maximized to fail in the specified failure sequence.

Maximization of Energy Absorption with Constraints for Separation Between Progressive Failure Modes

The optimum design obtained from the reliability optimization for progressive failure response of the laminate revealed that it is important to eliminate occurrence of multiple *failure modes* rather than constrain *ply failure events*. This requires that the objective function (energy absorption) be penalized only when two distinctly different failure modes occur at the same strain level. Two slightly different approaches, namely maximization of energy with failure mode separation and maximization of energy with constraint on the minimum strain separation, are used to find an optimum design, both based on the strain separation function from Eq. (8).

Maximization of Energy with Failure Mode Separation

The objective function for optimization with constraints on strain separation between failure modes is as follows:

$$\text{maximize}\left[\frac{E}{E_{\max}} - \frac{P_{\Delta\varepsilon}}{(P_{\Delta\varepsilon})_{\max}}\right] \tag{11}$$

The $P_{\Delta\varepsilon}$ term in the above strain separation penalty function is similar to the expression from Eq. (8), except now the summation is over the failure modes rather than the ply failure events. This penalty function does not prevent multiple plies of the same orientation from failing in identical failure modes at the same strain level. The rationale behind this is that for this in-plane problem, plies of the same orientation failing in the same mode do not result in different load distributions when the order of the ply failure changes. However, if the mode of failure changes then the resulting stiffness degradation and the load redistribution also change. For the optimization results presented here, the values used for the penalty function weighting term p_ε and minimum allowable delta strain $\Delta\varepsilon_{\min}$ were obtained by trial and error ($p_\varepsilon = 2$ and $\Delta\varepsilon_{\min} = 0.005$). The value of $(P_{\Delta\varepsilon})_{\max}$ was found by maximizing the value of the strain separation term [Eq. (9)] and it was found to be $(P_{\Delta\varepsilon})_{\max} = 9.009$. The best design for the failure event separation study is presented in Fig. 14.

A comparison of the 95% reliability energy absorption limit of the design obtained by enforcing strain separation between failure modes (Fig. 14), the design obtained from optimization using constraints for strain separation of ply failure events (Table 5) and the design obtained from reliability optimization (Table 8) when subjected to increasingly random ply angle variations is presented in Table 9.

The design obtained from reliability optimization provided the best balance between maximizing energy absorption and maximizing robustness. The design obtained from optimization of maximum energy absorbed with constraints for failure mode separation using the reformulated strain penalty function shows an improvement over the design in which mode separation was achieved by separating ply failures. This indicates that the reformulated approach is more efficient in separating competing failure modes. It is to be remembered that the strain separation limit between failure events and the penalty function weighting terms were chosen arbitrarily with a few trial and error changes. More investigation is needed to specify strain separation based on the interaction between the failure modes.

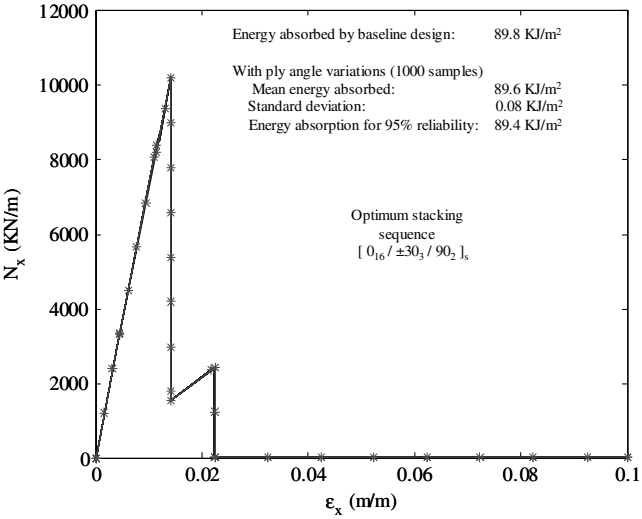

Fig. 14 Progressive failure of laminate optimized with constraint for strain separation between different failure modes when analyzed with ply angle variation of 0.1-deg standard deviation.

Maximization of Energy with Constraint on the Minimum Strain Separation

The penalty function previously used to enforce strain separation between failure modes summed the violation of the strain separation constraint over the progressive failure history. Here, we use an alternative approach in which the minimum strain separation between failure modes is constrained to be larger than a specified limit. The resulting objective function of the optimization is as follows:

$$\text{maximize}\left[\frac{E}{E_{\max}} - p_\varepsilon\left\langle 1 - \left(\frac{\varepsilon_x^i - \varepsilon_x^{i-1}}{\Delta\varepsilon_{\min}}\right)\right\rangle_{\max}\right] \tag{12}$$

where the bracket term $\langle\,\rangle_{\max}$ represents the maximum value of the strain separation penalty function (minimum strain difference) found between any two consecutive failure events of different modes. The values of the parameters used for this case were $p_\varepsilon = 2$ and $\Delta\varepsilon_{\min} = 0.005$. The deterministic design obtained by implementing this approach is shown in Table 10.

It can be seen that the new design consists of just 0-deg plies (which fail all at once in fiber mode). When using this approach, the optimization tends to converge toward a design that consists of plies with the same orientation, in which all plies fail at once and for which the minimum strain difference has a bigger value than $\Delta\varepsilon_{\min}$ (i.e., no strain penalty is applied). Basically, all competing failure modes are eliminated because the progressive failure of the deterministic design (Table 10) consists of just one failure event (i.e., there are no multiple failure modes that can compete with each other). The limit for 95% reliability hardly changes when angle variations are incremented. Although all the way from angle variations with 0.1-deg standard deviation to 1-deg standard deviation the design shown in Table 10 has lower performance when compared with the design obtained by performing strain separation between failure modes (last row in Table 9), the performance of the $[0_{24}]_s$ laminate is best obtained thus far when large angle variations with 1.66-deg standard deviation are introduced (86.1 KJ/m^2 vs 83.3 KJ/m^2).

Both approaches used for eliminating competing failure modes were successful in improving failure predictability. It can be seen from Fig. 14 that the failure progressions of the deterministic design with and without small ply angle variations are almost identical. This

Table 9 Comparison of the energy absorption limit for 95% reliability for designs with failure event separation in different modes, ply failure separation, and design from reliability optimization

Optimization criteria and stacking sequence of optimum laminate design	Energy absorbed by nominal design, KJ/m^2	Energy absorption limit (KJ/m^2) for 95% reliability under random normal ply orientation angle variations with standard deviation of				
		0.1 deg	0.2 deg	0.3 deg	1.0 deg	1.66 deg
Reliability optimization for maximizing energy absorption limit of 95% reliability (for normal random ply angle variations with 1-deg standard deviation) $[\mathbf{0_{18}}/\pm\mathbf{30}/\pm\mathbf{45}/\pm\mathbf{60}]_s$	90.2	93.5 (93.76, 0.09)[a]	93.1	92.7	90.5	89.3
Optimization for maximum energy absorption with constraint for strain separation between *ply failure events* $[\mathbf{0_{12}}/\pm\mathbf{30_4}/\pm\mathbf{60}/\pm\mathbf{90_2}]_s$	95.6	87.1 (87.3, 0.10)[a]	86.6	86.1	82.6	80.6
Optimization for maximum energy absorption with constraint for strain separation between *failure modes* $[\mathbf{0_{16}}/\pm\mathbf{30_3}/\pm\mathbf{90_2}]_s$	89.8	89.4 (89.9,0.08)[a]	88.7	87.9	86.3	83.3

[a]Values in parenthesis are the mean and standard deviation of the energy absorbed by the laminates with small random ply angle variation.

Table 10 Variation of energy absorption limit for 95% reliability for design obtained using the minimum strain separation value to penalize the energy absorption

Optimization criteria and stacking sequence of optimum laminate design	Energy absorbed by design, KJ/m^2	Energy absorption limit (KJ/m^2) for 95% reliability under random normal ply orientation angle variations with standard deviation of				
		0.1 deg	0.2 deg	0.3 deg	1.0 deg	1.66 deg
Design obtained by performing *failure event separation* using the minimum strain separation value $[\mathbf{0_{24}}]_s$	86.3	86.3 (86.3, 0.0003)[a]	86.3	86.3	86.2	86.1

[a]Values in parenthesis are the mean and standard deviation of the energy absorbed by the laminates with small random ply angle variation.

is reflected in the similarity among values of the energy absorbed by baseline design (89.8 KJ/m^2), main energy absorbed (89.6 KJ/m^2) and the 95% reliability (89.4 KJ/m^2). Although the design obtained from reliability optimization has the best 95% reliability value among all designs examined, the reformulated methodology for separating failure modes proved that designs with similar performance and robustness can be obtained for a fraction of the computational effort required to perform a reliability optimization study.

Conclusions

The progressive failure behavior of composite laminates was investigated and it was shown to have many similarities to progressive failure of complex structures and systems. The effect of optimization on reducing predictability of failure was demonstrated. The maximization of energy absorption using deterministic optimization produced a design with very poor robustness. The optimum design when subjected to small random variations (normally distributed with zero mean and 0.1-deg standard deviation) exhibited significant change in its failure sequences and a large reduction in the energy absorption. The optimized design was shown to be more sensitive to small random variations than an optimized quasi-isotropic design (i.e., less robust). Investigation of the optimized design revealed that the underlying reason to this sensitivity is the coalescence of multiple failure modes to the same strain (loading) level. In such cases, even small changes to design variables or loads lead to changes in the order in which the failure modes occur. Changes in the failure modes result in significant changes in stiffness degradations, residual strengths, and the load redistribution among the plies that have not failed. In essence, the coalesced modes interact with each other and result in bifurcations that lead to competing failure paths.

A deterministic optimization procedure was developed to maximize energy absorption and eliminate competing failure modes. Two different approaches were investigated to achieve strain separation between the failure modes. Both were indirect methods that simply enforced strain separation between ply failure events and restricted the load drop at any failure event. The approach was effective in separating modes and improving failure predictability of the optimized designs. A reliability optimization was performed for the same example. The reliability optimization was able to improve the reliability of the design for small ply angle variations but did not eliminate the competing failure paths. Therefore, the design is less robust when the ply angle variations are increased by a small amount from the value it was optimized for. Reliability optimization for large random variations provided a more robust design that did not have competing failure modes and also had higher energy absorption compared with the design obtained with separation between ply failure events. A comparison of the designs indicated that to eliminate competing failure paths it is more important to have strain separation between failure modes. That means that plies of different orientations must not fail at the same strain level and plies of the same orientation must not fail in different modes. A deterministic optimization with constraints to enforce strain separation between failure modes (not ply failures) was implemented. The optimum design obtained had a high energy absorption value and yet provided highly robust progressive failure response and predictable failure sequence.

Acknowledgments

This research was supported by grants from San Diego State University Research Foundation and from Northrop Grumman Corporation. The authors also wish to thank Raphael T. Haftka at the University of Florida for many useful discussions regarding this work.

References

[1] Belytschko, T., and Mish, K., "Computability in Non-Linear Solid Mechanics," *International Journal for Numerical Methods in Engineering*, Vol. 52, 2001, pp. 3–21.

[2] Murri, G. B., Schaff, J. R., and Dobyns, A. L., "Fatigue Life Analysis of Hybrid Composite Tapered Flexbeams," *Proceedings of the 14th International Conference on Composite Materials*, 2003.

[3] Vandeperre, L. J., and Van Der Biest, O. O., "Graceful Failure of Laminated Ceramic Tubes Produced by Electrophoretic Deposition," *Journal of the European Ceramic Society*, Vol. 18, No. 13, 1998, pp. 1915–1921.

[4] Roux, W. J., Stander, N., Guenther, G., and Muelllershoen, H., "Stochastic Analysis of Highly Nonlinear Structures," *International Journal for Numerical Methods in Engineering*, Vol. 65, No. 8, 2005, pp. 1221–1242.

[5] Lyle, K., Fasanella, E., Melis, M., Carney, K., and Gabrys, J., "Application of Non-Deterministic Methods to Assess Modeling

Uncertainties for Reinforces Carbon–Carbon Debris Impacts," *Proceedings of the 8th International LS-DYNA Users Conference*, 2004, pp. 3.23–3.34.

[6] Blumhardt, R., "FEM: Crash Simulation and Optimization," *International Journal of Vehicle Design*, Vol. 26, No. 4, 2001, pp. 331–347.

[7] Thole, A.-A., and Liguan, M., "Reasons for Scatter in Crash Simulation Results," *Proceedings of the 4th European LS-DYNA Conference*, 2003.

[8] Soden, P. D., Hinton, M. J., and Kaddour, A. S., "A Comparison of the Predictive Capabilities of Current Failure Theories for Composite Laminates," *Composites Science and Technology*, Vol. 58, 1998, pp. 1225–1254.

[9] Thompson, J. M. T., and Supple, W. J., "Erosion of Optimum Designs by Compound Branching Phenomena," *Journal of the Mechanics and Physics of Solids*, Vol. 21, 1973, pp. 135–144.

[10] Bertram, J. E. A., and Biewener, A. A., "Bone Curvature: Sacrificing Strength for Load Predictability," *Journal of Theoretical Biology*, Vol. 131, 1998, pp. 75–92.

[11] Reilly, G., and Currey, J. D., "The Development of Microcracking and Failure in Bone Depends on the Loading Mode to Which They Are Adapted," *Journal of Experimental Biology*, Vol. 202, No. 5, 1999, pp. 543–552.

[12] Sarraf, M., and Bruneau, M., "Ductile Seismic Retrofit of Steel Deck-Truss Bridges, 1: Strategy and Modeling," *Journal of Structural Engineering*, Vol. 124, No. 11, 1998, pp. 1253–1271.

[13] Kim, H. S., and "Wierzbicki, T., "Effect of the Cross-Sectional Shape of Hat-Type Cross Sections on Crash Resistance of an "S" Frame," *Thin-Walled Structures*, Vol. 39, 2001, pp. 535–554.

[14] Pedersen, P., "Topology Optimization Design of Crushed 2-D frames for Desired Energy Absorption History," Danish Center for Applied Mathematics, Technical Univ. of Denmark, Rept. 666, 2001.

[15] Zimmerman, J. J., and Corotis, R. B., "Stochastic Programs for Identifying Critical Structural Collapse Mechanisms," *Applied Mathematical Modelling*, Vol. 15, No. 7, 1991, pp. 367–373.

[16] Mahadevan, S., and Liu, X., "Probabilistic Optimum Design of Composite Structures," *Journal of Composite Materials*, Vol. 32, No. 1, 1998, pp. 68–82.

[17] Mahadevan, S., and Liu, X., "Probabilistic Analysis of Composite Structure Ultimate Strength," *AIAA Journal*, Vol. 40, No. 7, 2002, pp. 1408–1414.

[18] Cox, S. E., Haftka, R. T., Baker, C. A., Grossman, B., Mason, W. H., and Watson, L. T., "A Comparison of Global Optimization Methods for the Design of a High-Speed Civil Transport," *Journal of Global Optimization*, Vol. 21, 2001, pp. 415–433.

[19] Sobieszczanski-Sobieski, J., Kodiyalam, S., and Yang, R. J., "Optimization of Car Body Under Constraints of Noise, Vibration and Harshness (NVH) and Crash," *Structural and Multidisciplinary Optimization*, Vol. 22, 2001, pp. 295–396.

[20] Venkataraman, S., and Haftka, R. T., "Structural Optimization: What Has Moore's Law Done for Us?," *Structural and Multidisciplinary Optimization*, Vol. 28, No. 6, 2004, pp. 375–387.

[21] Hyer, M. W., *Stress Analysis of Fiber-Reinforced Composite Materials*, McGraw–Hill, New York, 1997.

[22] Padhi, G. S., Shenoi, R. A., Moy, S. S. J., Hawkins, G. L., "Progressive Failure and Ultimate Collapse of Laminated Composite Plates in Bending," *Composite Structures*, Vol. 40, Nos. 3–4, 1998, pp. 277–291.

[23] Ambur, D. R., Jaunky, N., Hilburger, M., and Davila, C. G., "Progressive Failure Analyses of Compression-Loaded Composite Curved Panels With and Without Cutouts," *Composite Structures*, Vol. 65, No. 2, 2004, pp. 143–155.

[24] Melchers, R. E., *Structural Reliability Analysis and Prediction*, Wiley, New York, 1999.

[25] McMahon, M. T., Watson, L. T., Soremekun, G. A., Gurdal, Z., and Haftka, R. T., "A Fortran 90 Genetic Algorithm Module for Composite Laminate Structure Design," *Engineering with Computers*, Vol. 14, 1998, pp. 260–273.

[26] Le Riche, R., and Haftka, R. T., "Optimization of Laminate Stacking Sequence for Buckling Load Minimization by Genetic Algorithm," *AIAA Journal*, Vol. 31, No. 5, 1993, pp. 951–956.

[27] Schutte, J. F., and Haftka, R. T., "Improved Global Convergence Probability Using Independent Swarms," AIAA Paper 2005-1896, Apr. 2005.

A. Roy
Associate Editor